Selectivity for CO$_2$ over CH$_4$ on a Functionalized Periodic Mesoporous Phenylene-Silica Explained by Transition State Theory

Christian Kunkel [a], Francesc Viñes [a], Mirtha A. O. Lourenço [b], Paula Ferreira [b], José R. B. Gomes [c,*] and Francesc Illas [a,*]

[a] *Departament de Ciència dels Materials i Química Fisica & Institut de Química Teòrica i Computacional (IQTCUB), Universitat de Barcelona, Martí i Franqués 1-11, 08028 Barcelona, Spain.*

[b] *Department of Materials & Ceramics Engineering, CICECO, University of Aveiro, 3810-193 Aveiro, Portugal.*

[c] *Department of Chemistry, CICECO, University of Aveiro, 3810-193 Aveiro, Portugal.*

*Corresponding authors: jrgomes@ua.pt , francesc.illas@ub.edu

Graphical abstract
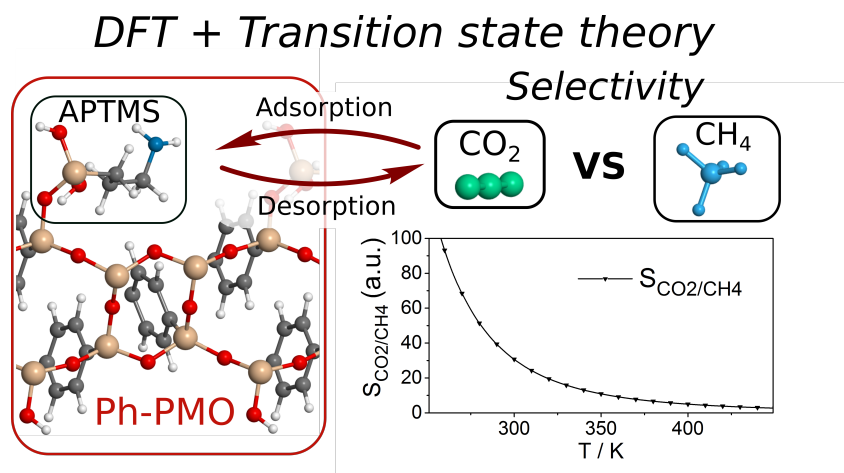
Keywords

Periodic mesoporous organosilicas - PMO, CO_2/CH_4 separation, Transition state theory, DFT

Highlights

- We study the interaction of functionalized periodic mesoporous phenylene-silica APTMS@Ph-PMO with CO_2 and CH_4 by dispersion corrected periodic density functional theory (DFT).

- From a transition state theory based approach using such DFT results, an estimation of initial CO_2/CH_4 selectivity is presented for a wide temperature range.

- At ambient temperatures (298 K), such determined CO_2/CH_4 selectivity of 32.2 agrees to a value of 26.1 from previous experiments

Abstract

Separation of CO_2/CH_4 is critical in biogas upgrading, necessitating materials with high selectivity. Here we simulate it for functionalized periodic mesoporous phenylene-silica material APTMS@Ph-PMO: Dispersion corrected density functional theory calculations are carried out to study the interaction of APTMS@Ph-PMO with CO_2 and CH_4, yielding most stable adsorption energies of -0.30 and -0.14 eV respectively. Relying on these DFT results, (ad)desorption rates are gained from transition state theory allowing for the estimation of initial CO_2/CH_4 selectivities at various temperatures. At 298 K selectivity of 32.2 agrees to an experimental value of 26.1, validating the methodology to evaluate CO_2/CH_4 adsorption selectivities.

Main text

The production of biogas from anaerobic decomposition of organic matter has been proposed as a viable source of renewable energy helping in satisfying the rising world energy demand. Biogas contains mainly methane (50-75%) and carbon dioxide (25-50%) [1], and traces of H_2S, CO, H_2, and N_2 [1,2]. Since impurities may cause corrosion, deposits, and damage to equipment, the complete removal of contaminant species from

biogas is required to produce biomethane. Especially CO_2 removal is critical if the biogas is to be upgraded for household applications (standard natural gas) or car fuels, since a high fraction of CO_2 reduces the energy content [3–8]. For example, to introduce the biogas at the natural gas pipelines methane needs to present a level of purification of 97 %, requiring energy efficient processes for CO_2 separation from CH_4 [9,10]. Thus, strong efforts are being made to develop materials for the separation of these gases [11]. Conventional adsorbents with different composition and structure such as activated carbons [12–16], zeolites [9,12,17–20], clays [21,22], metal organic frameworks (MOFs) [12,23,24], and mesoporous silica-based materials [25,26] have been proposed, but showed low separation performances.

In recent studies some of the authors have been evaluating the use of functional periodic mesoporous phenylene-silicas (Ph-PMOs) as adsorbents for CO_2/CH_4 gas separation since they present high specific surface areas, high pore volumes, and high thermal stability [27–29]. Additionally, Ph-PMOs display a narrow distribution of both meso- and molecular-scale periodicities; a clear advantage for adsorbate diffusion within the pore channels. Moreover, we have seen [30,31] that the modification of the Ph-PMO with amine groups allows the optimization of their properties for the separation of CO_2/CH_4, by improving the interaction with the CO_2 molecule. Recently, we demonstrated that aminopropyl groups grafted to the free silanols of Ph-PMO promote selectivity for CO_2/CH_4 separation making the resulting APTMS@Ph-PMO so far the most selective of all PMOs applied in this field, at 25 °C adsorbing 26.1 times more CO_2 than CH_4, as determined by the ratio of Henry constants [30].

Thus far, selectivity for CO_2/CH_4 separation for different functionalized PMOs has been evaluated by using experiments [30,31], while the CO_2 and CH_4 adsorption mechanisms involved in this materials were clarified using periodic density functional theory (DFT) calculations [30]. In fact, as we have observed, experimental gas adsorption data and computational studies are in good agreement and such DFT results proved also useful to guide the preparation of more efficient PMO materials. Motivated by these results, we are here assessing gas adsorption data by theoretical modeling, using results of DFT calculations including dispersive forces in combination with transition state theory. For a case study, we determine the rates of adsorption and desorption of CO_2 and CH_4 on

APTMS@Ph-PMO, allowing us to obtain CO_2/CH_4 selectivity over a wide temperature range. A comparison between the so determined selectivity with the experimentally obtained value previously reported [30] shows good agreement and justifies the used models and assumptions.

To study the interaction of CO_2 and CH_4 with the previously described slab model of APTMS@Ph-PMO [32], periodic DFT calculations have been carried out within the generalized gradient approximation (GGA) using the Vienna *ab initio* simulation package (VASP) [33]. Exchange-correlation effects were described using the Perdew-Burke-Ernzerhof (PBE) exchange-correlation (xc) functional, adding the van der Waals D2 dispersion correction as proposed by Grimme (PBE-D2) [34–36]. Further computational details are given in the Supplementary Content, restating here for a better understanding of the oncoming discussion that favorable adsorption energies, E_{ads} are defined negative and that interactions are more favorable for lower values of E_{ads}. As discussed elsewhere, the PBE-D2 method has proven suitable to describe small molecule adsorption on PMO models [32].

In a first step, stable adsorption sites for CO_2 and CH_4 on APTMS@Ph-PMO were identified by a screening of different starting positions for the gas phase molecules. In total, stable adsorption of CO_2 was found on 2 different sites, whereas 4 sites were identified for CH_4. In the oncoming discussion, these sites are numerated as P1-P4 and adsorption energies are given in Table 1. For a graphical depiction of geometries we refer to Table S1 of the Supplementary Content. The sites P1 and P2 both adsorb CO_2 and CH_4 and in fact P1 is as previously reported [30] the most stable adsorption site for both molecules with adsorption energies of -0.30 and -0.14 eV respectively. Adsorption energies on other sites are only slightly less favorable and competitive especially on P2 with -0.27 and -0.12 eV respectively or for CH_4 on P4 with -0.14 eV similarly stable as on P1. An expectable interaction strength is likely superimposed of contributions from all sites, possibly better captured by an average adsorption energy. For CO_2 and CH_4 this is given as -0.29 and -0.13 eV and the ratio of both being 2.23. With adsorption energies in this order of magnitude and geometries of adsorbed CO_2 and CH_4 only slightly differing from the gas phase molecules, the interaction can be safely described as physisorption.

Given that adsorption energies for CO_2 and CH_4 differ and that the interaction is more favorable for the former, there is clear interest for an estimation of selectivity by using DFT results. Here such an assessment is done from adsorption and desorption rates, which can be estimated in the framework of harmonic transition state theory (TST). Hence, for CO_2 and CH_4 adsorption and desorption rates have been calculated for temperatures from 40 to 1000 K with necessary quantities obtained from the above commented DFT calculations. The approach and equations are fully explained in the Supplementary Content. In short, the adsorption rate r_{ads}^{CO2} of CO_2 and r_{ads}^{CH4} of CH_4 depend on impingement of the gas phase molecule to the surface and therefore, on respective partial pressure (p_{CO2} or p_{CH4}). In total, adsorption rates for each of the two molecules have been calculated at five partial pressures, namely 0.05, 0.15, 0.5, 1.0, and 5.0 bars, thus allowing an assessment of the adsorption/desorption equilibrium over a wide pressure range, however with the restriction of model validity at higher pressures as discussed below. Desorption rates r_{des}^{PX} from each P1-P4 site differ in the employed model, due to dependence on adsorption energy and adsorbate vibrational frequencies. As above-mentioned, contributions from the identified sites could be superimposed and it seems reasonable to calculate average desorption rates r_{des}^{CO2} and r_{des}^{CH4} for CO_2 and CH_4, as

$$r_{des}^{CO2} = \frac{1}{2}(r_{des}^{P1} + r_{des}^{P2}) \qquad (1)$$

$$r_{des}^{CH4} = \frac{1}{4}(r_{des}^{P1} + r_{des}^{P2} + r_{des}^{P3} + r_{des}^{P4}) \qquad (2)$$

The so estimated adsorption and desorption rates are graphically given in Figure 1 a). Focussing first on the adsorption rates: Values for 0.05 bar partial CO_2/CH_4 pressure are given here whereas for higher partial pressures we refer to Figure S1 of the Supplementary Content. Overall, the CH_4 adsorption rate is higher by a factor of 1.7 compared to CO_2, understandable from the smaller CH_4 molar mass, see equation (2) in the Supplementary Content. It should thus be mentioned that the experimentally determined CO_2 selectivity of the APTMS@Ph-PMO at equal partial pressures is not explainable from adsorption rates.

Differing rates of CO_2 and CH_4 can thus likely better serve an explanation for observed selectivity. Focussing first on average desorption rates r_{des}^{CO2} and r_{des}^{CH4}, both curves significantly differ, with r_{des}^{CO2} showing lower values below a crossing temperature of 645

K. A CO_2 selectivity over CH_4 is thus possible below this fringe temperature, whereas towards higher temperatures could become reversed. We will further evaluate such selectivity, taking also into account the additional influence of adsorption rates, see below.

With rates of adsorption and desorption at hand, fringe temperatures can now be assessed, below which adsorption prevails and consequently, CO_2 or CH_4 accumulates on the material. Such a temperature fringe is to be found when desorption starts to exceed adsoption. For CH_4 at 0.05 bar partial pressure this likely happens in the range of the intersection temperatures $T_1 = 55$ K. For CO_2 this temperature is shifted to higher values of $T_2 = 145$ K in congruence with higher adsorption energy. These fringe temperatures rise for higher partial pressures, see Figure S1 of the Supplementary Content though in all cases are found below ambient temperatures. A note of caution should be added when comparing with higher pressures, as coverage dependence is not accounted for in this approach, obtained rates better correlate with the low pressure behaviour of the material.

From the obtained data, an estimate of low coverage CO_2 to CH_4 selectivity $S_{CO2/CH4}$ is interesting, allowing comparison to the experimentally determined value. Thus, the equilibrium constants of adsorption and desorption for CO_2, K_{CO2} and CH_4, K_{CH4} are set in relation, allowing a definition of $S_{CO2/CH4}$ as

$$S_{CO2/CH4} = \frac{K_{CO2}}{K_{CH4}} \tag{3}.$$

These equilibrium constants are in turn defined as

$$K_{MX_n} = \frac{r_{ads}^{MX_n}}{r_{des}^{MX_n}}; \quad MX_n = CO_2 \text{ or } CH_4 \tag{4}.$$

where adsorption rates r_{ads}^{CO2} and r_{ads}^{CH4} used here had been evaluated at equal partial pressures of the gas phase molecules. In this form, $S_{CO2/CH4}$ captures material selectivity for a low pressure gas mixture of CO_2/CH_4 in a 50/50 ratio.

The obtained selectivity presented in Figure 1b, displays strong temperature dependence: Selectivity is predicted higher at lower temperatures, important for evaluation of an optimum CO_2 and CH_4 separation temperature from *e.g.* a biogas output stream. Given the predicted variation of $S_{CO2/CH4}$ with temperature, a simple evaluation of

selectivity by the ratio of adsorption energies (given as 2.23, see Table 1), could only serve as a first hint, with entropic effects then being neglected.

At 298 K, $S_{CO2/CH4}$ shows a of value 32.2, therefore in good agreement with a low pressure selectivity of 26.1 experimentally found from the ratio of Henry constants [30]. Such an agreement would not be surprising for solid surfaces, where TST is widely used for evaluation of adsorption and desorption rates [37], take applications to modelling of temperature programmed desorption for CO_2 [38] and CH_4 [39], in kinetic Monte Carlo simulations [40,41] and as a predictive tool [42]. The validity of the approach however was initially ambiguous for a mesoporous material like APTMS@Ph-PMO with an average pore size of approximately 2.5 nm [30]: Here, diffusive processes into pores could play an important role for selectivity but are initially not included in the model. However, the good agreement to experiment suggests that the initial capture on the exposed surface plays a determining role for selectivity, thus justifying the use of such a model. In fact, when small, influence of the subsequent diffusion into pores on adsorption rates could be rather simply accounted for by adjusting the sticking factor S_0 such as to capture pore entrance probability [43]. Here a conservative value was chosen, see also the further discussion in the Supplementary Content.

In conclusion, for the case study of functionalized periodic mesoporous phenylene-silicas material APTMS@Ph-PMO, the interaction of CO_2 and CH_4 was rationalized by periodic DFT at the PBE level with dispersion correction (PBE-D2). In total, two preferential adsorption sites were identified for CO_2 and four for CH_4 with most stable adsorption energies on the order of -0.30 and -0.14 eV respectively. Relying only on these DFT results, a herein presented transition state theory based approach allows a theoretical estimate of initial CO_2/CH_4 selectivity for the mesoporous APTMS@Ph-PMO over a wide temperature range. At temperatures of 298 K, the estimated selectivity of 32.2 agrees well with a value of 26.1 from previous experiments. As DFT results have previously been demonstrated to capture well the trends in selectivity for a series of functionalized Ph-PMOs, we propose this model for theory-driven evaluation of further modifications, possibly helping to achieve even higher CO_2/CH_4 selectivity.

Supplementary Content

The supplementary content contains computational details, calculated vibrational frequencies, top views of adsorbate structures, explanation of the used rate model, and adsorption rates at different partial pressures of CO_2 and CH_4 are presented therein.

Acknowledgments

References

[1]   T.Z.D. de Mes, A.J.M. Stams, J.H. Reith, G. Zeeman, in:, Bio-Methane Bio-Hydrogen, Status Perspect. Biol. Methane Hydrog. Prod., 2003, pp. 58 –102.

[2]   P. Jaramillo, H.S. Matthews, Environ. Sci. Technol. 39 (2005) 7365–7373.

[3]   M. Harasimowicz, P. Orluk, G. Zakrzewska-Trznadel, A.G. Chmielewski, J. Hazard. Mater. 144 (2007) 698–702.

[4]   E. Favre, R. Bounaceur, D. Roizard, J. Memb. Sci. 328 (2009) 11–14.

[5]   S. Heile, S. Rosenberger, A. Parker, B. Jefferson, E.J. McAdam, J. Memb. Sci. 452 (2014) 37–45.

[6]   X. Wu, M. Niknam Shahrak, B. Yuan, S. Deng, Microporous Mesoporous Mater. 190 (2014) 189–196.

[7]   K.S. Knaebel, H.E. Reinhold, Adsorption 9 (2003) 87–94.

[8]   A. Lohila, T. Laurila, J.P. Tuovinen, M. Aurela, J. Hatakka, T. Thum, M. Pihlatie, J. Rinne, T. Vesala, Environ. Sci. Technol. 41 (2007) 2717–2722.

[9]   S. Cavenati, C.A. Grande, A.E. Rodrigues, Energy Fuels 20 (2006) 2648–2659.

[10] Y.S. Bae, R.Q. Snurr, Angew. Chemie 50 (2011) 11586–11596.

[11] A.E. Rodrigues, C.A. Grande, Ind. Eng. Chem. Res. 46 (2007) 4595–4605.

[12] R. Babarao, Z. Hu, J. Jiang, S. Chempath, S.I. Sandler, Langmuir 23 (2007) 659–666.

[13] M.B. Kim, Y.S. Bae, D.K. Choi, C.H. Lee, Ind. Eng. Chem. Res. 45 (2006) 5050–5058.

[14] X. Peng, W. Wang, R. Xue, Z. Shen, AIChE J. 52 (2006) 994–1003.

[15] V. Goetz, O. Pupier, A. Guillot, Adsorption 12 (2006) 55–63.

[16] H. Yi, F. Li, P. Ning, X. Tang, J. Peng, Y. Li, H. Deng, Chem. Eng. J. 215-216 (2013) 635–642.

[17] S. Cavenati, C.A. Grande, A.E. Rodrigues, J. Chem. Eng. Data 49 (2004) 1095–1101.

[18] P. Li, F. Handan Tezel, Microporous Mesoporous Mater. 98 (2007) 94–101.

[19] J.-M. Leyssale, G.K. Papadopoulos, D.N. Theodorou, J. Phys. Chem. B 110 (2006) 22742–22753.

[20] E.L. First, M.M.F. Hasan, C.A. Floudas, AIChE J. 60 (2014) 31–33.

[21] M.L. Pinto, J. Pires, J. Rocha, J. Pys. Chem. C. 112 (2008) 14394–14402.

[22] J. Pires, V.K. Saini, M.L. Pinto, Environ. Sci. Technol. 42 (2008) 8727–8732.

[23] D.M. D'Alessandro, B. Smit, J.R. Long, Angew. Chemie - Int. Ed. 49 (2010) 6058–6082.

[24] G.D. Pirngruber, L. Hamon, S. Bourrelly, P.L. Llewellyn, E. Lenoir, V. Guillerm, C. Serre, T. Devic, ChemSusChem 5 (2012) 762–76.

[25] Q. Xue, Y. Liu, Sep. Sci. Technol. 46 (2011) 679–686.

[26] X. Liu, L. Zhou, X. Fu, Y. Sun, W. Su, Y. Zhou, Chem. Eng. Sci. 62 (2007) 1101–1110.

[27] T. Asefa, M.J. MacLachlan, N. Coombs, G.A. Ozin, Nature 402 (1999) 867–871.

[28] S. Inagaki, S. Guan, Y. Fukushima, T. Ohsuna, J. Am. Chem. Soc. 121 (1999) 9611–9614.

[29] B.J. Melde, B.T. Holland, C.F. Blanford, A. Stein, Chem. Mater. 11 (1999) 3302–3308.

[30] M.A.O. Lourenço, C. Siquet, M. Sardo, J. Pires, L. Mafra, M. Jorge, M.L. Pinto, P. Ferreira, J.R.B. Gomes, J. Phys. Chem. C 120 (2016) 3863–3875.

[31] M.A.O. Lourenço, C. Siquet, J. Santos, M. Jorge, J.R.B. Gomes, P. Ferreira, J. Phys. Chem. C 120 (2016) 14236–14245.

[32] M.A.O. Lourenço, C. Siquet, M. Sardo, L. Mafra, J. Pires, M. Jorge, M.L. Pinto, P. Ferreira, J.R.B. Gomes, J. Phys. Chem. C 120 (2016) 3863–3875.

[33] G. Kresse, J. Furthmüller, Phys. Rev. B 54 (1996) 11169–11186.

[34] J.P.P. Ramalho, J.R.B. Gomes, F. Illas, RSC Adv. 3 (2013) 13085.

[35]   S. Grimme, J. Comput. Chem. 27 (2006) 1787–1799.

[36]   J.L.C. Fajín, M.N. D. S. Cordeiro, J.R.B. Gomes, F. Illas, J. Chem. Theory Comput. 8 (2012) 1737–1743.

[37]   S.J. Lombardo, A.T. Bell, Surf. Sci. Rep. 13 (1991) 3–72.

[38]   R.S. Smith, Z. Li, L. Chen, Z. Dohnálek, B.D. Kay, J. Phys. Chem. B 118 (2014) 8054–8061.

[39]   S.L. Tait, Z. Dohnálek, C.T. Campbell, B.D. Kay, J. Chem. Phys. 122 (2005) 164708.

[40]   K. Reuter, M. Scheffler, Phys. Rev. B 73 (2006) 045433.

[41]   R.A. van Santen, A.J. Markvoort, I.A.W. Filot, M.M. Ghouri, E.J.M. Hensen, Phys. Chem. Chem. Phys. 15 (2013) 17038.

[42]   C. Kunkel, F. Viñes, F. Illas, Energy Environ. Sci. 9 (2016) 141–144.

[43]   J.-M. Simon, J.-P. Bellat, S. Vasenkov, J. Kärger, J. Phys. Chem. B 109 (2005) 13523–13528.

Table 1: Adsorption energies for CO_2 and CH_4 on the different sites of the APTMS@Ph−PMO model. E_{ads} are for PBE-D2 and given in eV with most stable sites highlighted in bold. Adsorbate geometries are given in the Supplementary Content.

	P1	P2	P3	P4	Avg.[a]
E_{ads} (CO_2)	**-0.30**	-0.27	–	–	-0.29
E_{ads} (CH_4)	**-0.14**	-0.12	-0.10	**-0.14**	-0.13
Ratio	–	–	–	–	2.23

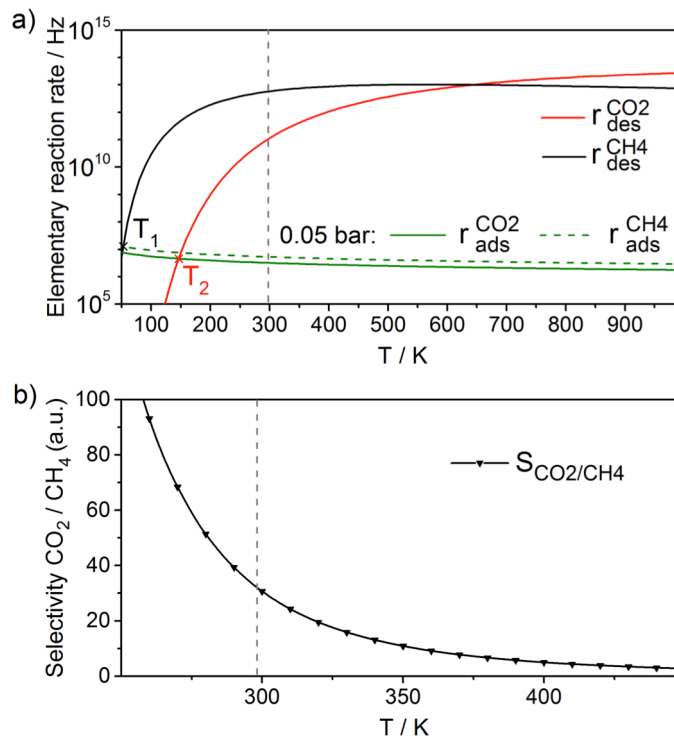[a] Average (arithmetic mean) of all adsorption energies for CO_2 or CH_4.

Figure 1: a) Temperature dependence for calculated rates of adsorption and desorption of CO_2 and CH_4 on the mesoporous APTMS@Ph-PMO material. b) Initial CO_2/CH_4 selectivity $S_{CO2/CH4}$. A vertical gray line in both graphs indicates ambient temperature (298 K).